HHS Public Access

Author manuscript

Neurobiol Aging. Author manuscript; available in PMC 2019 June 01.

Published in final edited form as:

Neurobiol Aging. 2018 June ; 66: 32–39. doi:10.1016/j.neurobiolaging.2018.02.001.

Multimodal Neuroimaging and Behavioral Assessment of SNCA Polymorphism rs356219 in Older Adults

Roxana G. Burciu, PhD[a], **Rachael D. Seidler, PhD**[a], **Priyank Shukla, PhD**[a], **Mike A. Nalls, PhD**[b,c], **Andrew B. Singleton, PhD**[b], **Michael S. Okun, MD**[c], and **David E. Vaillancourt, PhD**[a,d,f]

[a]Department of Applied Physiology and Kinesiology, University of Florida, Gainesville, FL, USA

Corresponding Author: David E. Vaillancourt, PhD, Department of Applied Physiology and Kinesiology, University of Florida, P.O. Box 118205, Gainesville, FL, 32611, Phone: 352-294-1770, vcourt@ufl.edu.

Author contributions:

- Roxana G. Burciu: research project execution, data processing and statistical analysis, manuscript preparation.
- Rachael D. Seidler: manuscript preparation.
- Priyank Shukla: data processing.
- Mike A. Nalls: manuscript preparation.
- Andrew B. Singleton: manuscript preparation.
- Michael S. Okun: manuscript preparation.
- David E. Vaillancourt: statistical analysis, manuscript preparation.

Financial disclosures:

- Dr. Roxana G. Burciu – Receives grant funding from NIH and Bachmann-Strauss Dystonia and Parkinson Foundation.
- Dr. Rachael D. Seidler – Reports grants from NIH, NSF, NASA, and the National Space Biomedical Research Institute during the conduct of the study, and personal honoraria from UTMB unrelated to the submitted work.
- Dr. Priyank Shukla – Reports no disclosures.
- Dr. Mike A. Nalls – Dr. Mike A. Nalls' participation is supported by a consulting contract between Data Tecnica International and the National Institute on Aging, NIH, Bethesda, MD,USA, as a possible conflict of interest Dr. Nalls also consults for Illumina Inc, the Michael J.Fox Foundation and University of California Healthcare.
- Dr. Andrew B. Singleton – Reports no disclosures.
- Dr. Michael S. Okun – Serves as consultant for the National Parkinson's Foundation, and has received research grants from the National Institutes of Health, National Parkinson's Foundation, Michael J. Fox Foundation, Parkinson Alliance, Smallwood Foundation, Bachmann-Strauss Foundation, Tourette Syndrome Association, and UF Foundation. Dr.Okun has previously received honoraria, but in the past > 60 months has received no support from industry. Dr. Okun has received royalties for publications with Demos, Manson, Amazon, Smashwords, Books4Patients, and Cambridge (movement disorders books). Dr.Okun is an associate editor for New England Journal of Medicine Journal Watch Neurology. Dr. Okun has participated in CME and educational activities on movement disorders (in the last 36 months) sponsored by PeerView, Prime, Quantia, Henry Stewart, and the Vanderbilt University. The institution and not Dr. Okun receives grants from Medtronic, Abbvie, and ANS/St. Jude, and the PI has no financial interest in these grants. Dr. Okun has participated as a site PI and/or co-I for several NIH, foundation, and industry sponsored trials over the years but has not received honoraria.
- Dr. David E. Vaillancourt – Reports grants from NIH, Bachmann-Strauss, and Tyler's Hope Foundation during the conduct of the study, and personal honoraria from NIH, National Parkinson's Foundation, UT Southwestern Medical Center, and Northwestern University unrelated to the submitted work. He is Co-Founder of Neuroimaging Solutions, LLC.

[b]Data Tecnica International, Glen Echo, MD, USA

[c]Laboratory of Neurogenetics, National Institute of Aging, Bethesda, MD, USA

[d]Department of Neurology, University of Florida, Gainesville, FL, USA

[e]Center for Movement Disorders and Neurorestoration, University of Florida, Gainesville, FL, USA

[f]Department of Biomedical Engineering, University of Florida, Gainesville, FL, USA

Abstract

The single nucleotide polymorphism rs356219 in the α-synuclein (SNCA) gene has been shown to significantly contribute to an earlier age at onset of Parkinson's disease (PD), regulate SNCA expression in PD-brain regions, blood and plasma. Here, we used multimodal MRI to study healthy adults with and without the rs356219 risk genotype. Motor and cognitive tests were administered and all participants underwent functional and structural MRI. Imaging analyses included: 1) task-based functional MRI, 2) task-based functional connectivity, 3) free-water diffusion MRI of the substantia nigra, 4) voxel-based morphometry, 5) surface-based morphometry. There were no differences between the two groups in motor and cognitive performance, or brain structure. However, carrying a PD risk variant was associated with reduced functional activity in the posterior putamen and primary motor cortex. Moreover, the posterior putamen had reduced functional connectivity with the motor cortex during motor control in those with a risk genotype compared to those without. These findings point to functional abnormalities in the striato-cortical circuit of rs356219 risk genotype carriers.

Keywords

SNCA; rs356219; MRI; basal ganglia; healthy

1. Introduction

The motor symptoms of Parkinson's disease (PD) have been the primary source for the clinical diagnosis of PD. (Brooks, 2012) It is also recognized that non-motor features are prominent early in PD, and could predate motor symptom onset. (Chaudhuri et al., 2006) The Movement Disorders Society has begun considering criteria for prodromal PD, and numerous contributory factors can put an individual at greater risk for PD. (Berg et al., 2015) One of the risk factors that has been identified is genetic history, including specific loci identified in genome-wide association studies that are associated with increased odds risk for PD. Despite knowing that older adults can carry a risk variant that places them at greater risk for developing PD, we are still just beginning to understand how being a carrier of a specific genetic risk variant affects key aspects of brain physiology in living humans.

Mutations in the α-synuclein (SNCA) gene have been known to cause autosomal dominant forms of PD (Biskup et al., 2008), while the risk of SNCA mutations in loci in sporadic PD have emerged from genome-wide association studies. (Lesage and Brice, 2012; Nalls et al., 2011) Among the single nucleotide polymorphisms (SNPs) in the SNCA gene associated with an increased risk of PD, the rs356219 SNP in particular has been shown to significantly

contribute to earlier age at onset of the disease, regulate SNCA expression in PD-brain regions, blood and plasma. (Brockmann et al., 2013; Fuchs et al., 2008; Lesage and Brice, 2012; Mata et al., 2010a; Nalls et al., 2014). Specifically, in a study that analyzed levels of α-synuclein in blood and human post mortem brain tissue showed that rs356219 had a significant effect on SNCA mRNA levels in the substantia nigra and cerebellum (Fuchs et al., 2008). In the current study, we use an approach that combines multimodal magnetic resonance imaging (MRI) and genetics to determine if healthy older adults that carry a risk genotype for SNCA rs356219 have imaging markers in the brain that mimic those of people with a diagnosis of PD. This approach is an important first step towards understanding the role of SNCA in brain function in health and disease.

Task-based functional magnetic resonance imaging (fMRI) and free-water diffusion magnetic resonance imaging (dMRI) have been identified as two key imaging markers for PD. Reduced fMRI signal in the putamen/posterior putamen has been repeatedly shown in cross-sectional motor control studies of PD patients compared with controls (Herz et al., 2013; Spraker et al., 2010). Recently, a longitudinal task-fMRI study indicated reduced signal in the putamen and primary motor cortex (M1) with the progression of PD. (Burciu, et al., 2016) Furthermore, studies have shown that the functional connectivity of the putamen with other regions of the brain is disrupted in PD patients compared to healthy controls. (Rieckmann et al., 2015; Tessitore et al., 2014) As for structural MRI changes, work from our group has shown that elevated free-water (FW) derived from diffusion MRI occurs in the posterior substantia nigra of early stage PD, as well as newly diagnosed de novo PD (Burciu et al., 2017; Ofori et al., 2015a), and in the anterior and posterior substantia nigra of moderate stage PD and parkinsonian syndromes. (Planetta et al., 2016) Moreover, it was found that FW levels in the posterior substantia nigra continue to increase with the progression of PD over the course of one, two, and four years. (Burciu et al., 2017; Ofori et al., 2015b) By contrast, cortical structural changes are not the hallmark of PD, and any abnormalities observed in the integrity of the cerebral cortex have often been linked to the later stages of the disease and/or cognitive dysfunction. (Chen et al., 2017; Rektorova et al., 2014)

In the current hypothesis-testing study, we used multimodal MR imaging and several motor and cognitive tests to study healthy older adults that carry a rs356219 risk genotype. The SNP examined was selected apriori based on its clear association with increased odds of developing PD. (Fuchs et al., 2008; Li. et al., 2013; Mata et al., 2010b; Nalls et al., 2015b; Nalls et al., 2014; Pan et al., 2012) Based on the recent evidence showing deficits in dopaminergic transmission that precede cell death and motor dysfunction in an α-synuclein transgenic mouse model (Janezic et al., 2013), we hypothesized that individuals carrying a PD risk genotype will present with functional abnormalities of the basal ganglia circuitry without structural brain changes or overt motor symptoms compared with individuals with a low risk, normal genotype.

2. Materials and Methods

2.1. Participants

A total of 31 older adults were tested in this study. They were recruited using advertisements from the local and surrounding communities in North Central Florida, and had no history of neuropsychiatric or neurological problems. Importantly, structural imaging was used to rule out microstructural brain abnormalities. The testing protocol included structural and functional brain imaging, and motor and cognitive tests. Genotyping was available for all participants and used to group people into those who had a risk genotype and those who had a normal genotype based on the SNP rs356219 of the SNCA gene (Table 1). The study was approved by the Institutional Review Board at the University of Florida, and all participants provided informed consent prior to data collection.

2.2. Genotyping using NeuroX

The NeuroX platform was used for genotyping (Nalls et al., 2015a). Genotyping was executed as per the manufacturer's protocol (Illumina, Inc). Our genotype calling workflow used a publicly available cluster file for the exome array standard content, which we modified to maximize variant calling for the NeuroX custom content. NeuroX comprises a backbone of standard Illumina exome content of approximately 240,000 variants, and over 24,000 custom content variants focusing on neurologic diseases. Standard GWAS quality control was undertaken with inclusion criteria such as a minimum call rate of 95% for participants and SNPs, a minor allele frequency of > 0.01, a Hardy-Weinberg equilibrium P value of > 1 × 10-7, no first-degree relatives in the sample collection (identity-by-descent score < 0.125 in PLINK) and European ancestry confirmed by multidimensional scaling analyses. For the SNP of interest, rs356219, the genotype for each individual was found in the NeuroX spreadsheet. If a subject was a carrier of at least one risk allele he/she was assigned to the risk genotype group (N=18), whereas if a subject did not have a risk variant he/she was assigned to the normal genotype group (N=13).

2.3. Clinical measures

Motor symptoms were assessed using part III of the Movement Disorder Society Unified Parkinson's Disease Rating Scale (MDS-UPDRS-III). (Goetz et al., 2008) We also evaluated bimanual coordination using the Purdue Pegboard Test as the total number of pins placed on the pegboard within 1 minute with both hands working simultaneously, and gait using the Dynamic Gait Index (DGI). (Desrosiers et al., 1995; Shumway-Cook et al., 1997) Cognitive status and the existence and severity of depression were measured with the Montreal Cognitive Assessment (MoCA) (Nasreddine et al., 2005) and Beck Depression Inventory, respectively. (Beck et al., 1961)

2.4. Acquisition of MR images

MR imaging was performed on a 3T Philips Achieva (Best, The Netherlands) MRI system equipped with a 32-channel SENSE head coil. We collected: 1) functional scans using a T_2*-weighted, single shot, echo-planar pulse sequence with repetition time=2500 ms, echo time=30 ms, flip angle=80°, field of view=240×240 mm, acquisition matrix=80×80, voxel

size=3 mm isotropic with no gap between slices (N=46); 2) whole brain diffusion imaging data using a single-shot spin echo EPI sequence: repetition time=7748 ms, echo time = 86 ms, flip angle=90°, field of view=224×224 mm, voxel size=2 mm isotropic with no gap between slices (N=60), diffusion gradient (monopolar) directions=64, diffusion gradient timing DELTA/delta=42.4/10 ms, *b*-values: 0, 1000 s/mm^2, fat suppression using SPIR, in-plane, SENSE factor=2; and 3) high-resolution structural data using a 3D T_1-weighted sequence with repetition time=8.2 ms, echo time=3.7 ms, flip angle=8°, field of view=240×240 mm, acquisition matrix=240×240, voxel size=1 mm isotropic with no gap between slices (N=170). To rule out microstructural brain abnormalities, we also acquired a T2-weighted scan: repetition time=7.0 ms, echo time=54 ms, flip angle=22°, field of view=224×224 mm, acquisition matrix=224×224, voxel size=1 mm isotropic with no gap between slices (N=64).

2.5. fMRI task: unimanual grip force

The task is well established in PD and is thoroughly detailed elsewhere. (Burciu, et al., 2016; Neely et al., 2015; Spraker et al., 2010). Prior to entering the MRI scanner, all participants were trained on the task and had their maximum voluntary contraction (MVC) measured using a pinch grip. The MVC was used to set the same target force level for all participants (i.e., 15% MVC). The fMRI protocol consisted of a block-design that alternated force and rest blocks as follows: 30s rest, 30s force with performance feedback, 12.5s rest, and 30s force without performance feedback. (Burciu et al., 2015; Neely et al., 2015; Spraker et al., 2010) This sequence was repeated four times and there was an additional 30s rest period following the final block of force without performance feedback. The task was visually guided and involved repetitive contraction and relaxation of hand muscles. A green cue was the go-signal for pushing on the force sensor and sustaining force (2 s), while red indicated a rest period (1 s). Hand use was balanced within groups to avoid a potential influence of hand response/dominance on the behavioral and imaging results.

2.6. Force data analysis

Data analysis procedures were consistent with the methodology used in our previous work. (Neely et al., 2013; Planetta et al., 2015) Force output was filtered using a 10th order Butterworth filter with a cutoff frequency of 15 Hz, and three variables were calculated: (1) mean force during the hold period expressed as % MVC, (2) mean rate up - the rate of change of increasing force across the ramp period, and (3) mean rate down - the rate of change of decreasing force across the relaxation period.

2.7. MRI data analysis

2.7.1. Task-based fMRI—Consistent with previous studies, the fMRI and T_1-weighted scans of those participants who performed the task with their left hand were flipped along the midline prior to preprocessing. (Burciu et al., 2015; Neely et al., 2015; Spraker et al., 2010) Data preprocessing was performed using Analysis of Functional NeuroImages (AFNI, https://afni.nimh.nih.gov/), and included the following steps: removal of the first four volumes of the functional scan to allow for T_1 equilibration effects; slice timing and head motion correction; normalization of the signal in each voxel at each time point by the mean

of its time series; registration of each volume of the functional data set to its first volume; co-registration of the functional scan with the structural scan; spatial normalization of the structural scan to the MNI_{152} template; reslicing of the functional scan in MNI space using the normalization parameters from the previous step; smoothing of the functional scan with a Gaussian kernel of 4 mm full width at half-maximum FWHM. Finally, fMRI data were regressed to a simulated hemodynamic response function for the task sequence (using the 3dDeconvolve function in AFNI), and percent signal change was calculated for each TR. Of note, the signal at each TR was averaged across force, consistent with previous studies. (Burciu, et al., 2016; Spraker et al., 2010) We calculated a mean percent signal change across 6 TRs toward the end of the task. This time interval was selected based on previous results showing a significant group (controls vs. PD) by TR interaction with task progression in nuclei of the basal ganglia (Spraker et al., 2010), and was confirmed to be sensitive to disease progression in a longitudinal fMRI study. (Burciu, et al., 2016) The regions used for the percent signal change analysis were the posterior putamen derived from the putamen ROI included in the Basal Ganglia Human Area Template (BGHAT) (Prodoehl et al., 2008), and M1 extracted from the Human Motor Area Template (HMAT) (Mayka et al., 2006), all contralateral to the hand tested. We also included a control ROI, a region responsible for complex non-motor functions which is not typically affected in PD. (Seghier, 2013) The control ROI was the contralateral angular gyrus and it was extracted from the Automated Anatomical Labeling Template (AAL). (Tzourio-Mazoyer et al., 2002)

2.7.2. Task-based functional connectivity—The analysis was carried out in AFNI and just like the task-based analysis it used AFNI's afni_proc.py scripting algorithm. Importantly, time series were further processed using ANATICOR in AFNI to extract spurious or nonspecific sources of variance from the BOLD data. These sources included the 6 motion parameters that describe rigid-body registration, white matter and cerebrospinal fluid, and the average signal across all voxels in the brain (i.e., global signal). Seeds were placed in the ROIs where percentage signal change differed with rs356219 genotype. Pearson correlations were computed between the seed and other voxels in the brain. The correlation maps were then converted to a Z-score.

2.7.3. Free-water diffusion MRI—The FMRIB Software Library (FSL, http://www.fmrib.ox.ac.uk/fsl/) and custom UNIX shell scripts were used to preprocess the data. First, scans were eddy current and head motion corrected. Gradient orientations were compensated to account for any rotation applied to the images, and non-brain tissue was removed. FW maps were calculated from the corrected volumes using a custom code written in MATLAB R2013a (The Mathworks, Natick, MA). (Ofori et al., 2015a; Ofori et al., 2015b) Briefly, a bi-tensor model was applied, where signal attenuation is computed from two compartments: one that models tissue and another that models FW. Next, the *b*0 images were normalized to a MNI-T_2 template by an affine transformation with 12 degrees of freedom and trilinear interpolation. The spatial transformation parameters obtained from this step were applied to the FW maps. Finally, for each participant, ROIs corresponding to the left and right posterior substantia nigra were hand-drawn on the normalized *b*0 image, and blinded to group status according to genotype, and blinded to the FW image. Consistent with

previous FW studies, we averaged FW across the left and right posterior substantia nigra. (Ofori et al., 2015a; Ofori et al., 2015b; Planetta et al., 2016)

2.7.4. Voxel-based morphometry—The voxel-based morphometry (VBM) analysis was performed using the Computational Anatomy Toolbox (CAT12, http://dbm.neuro.uni-jena.de/cat/) which runs in Statistical Parametric Mapping 12 (SPM12, http://www.fil.ion.ucl.ac.uk/spm/software/spm12/). Briefly, T_1-weighted images were corrected for signal intensity non-uniformities, segmented into tissue classes (gray matter - GM, white matter - WM, cerebrospinal fluid - CSF), spatially normalized using the DARTEL algorithm, modulated in order to obtain the absolute volume of GM tissue corrected for individual brain sizes, and smoothed with a Gaussian kernel of 8 mm FWHM. For exclusion of artefacts on the GM-WM border (i.e., incorrect voxel classification), we applied a GM threshold of 0.2.

2.7.5. Surface-based morphometry—For surface-based morphometry (SBM), we used the surface-preprocessing pipeline implemented in the CAT12 toolbox which extracts the cortical surface and quantifies cortical thickness based on an absolute mean curvature approach. (Dahnke et al., 2013; Luders et al., 2006) The T_1-weighted images were segmented into tissue classes to estimate WM distance, and the resulting WM distance maps were used to project the maximum local WM distance that is equivalent to the local thickness to other voxels. The left and right central cortical surfaces were reconstructed separately. Finally, for between-group comparisons, the left and right cortical thickness maps were resampled into a common coordinate system and smoothed with a Gaussian kernel of 15 mm FWHM.

2.8. Statistical analyses

First, Hardy-Weinberg equilibrium for rs356219 was tested using the Online Encyclopedia for Genetic Epidemiology HWE tool (OEGE). (Rodriguez et al., 2009) Next, we evaluated group differences in age and sex using an independent-samples *t*-test and Pearson Chi-Square, in order to determine if the upcoming statistical analyses should include these measures as covariates. Since there were no differences in age or sex (*p values* listed in Table 1) between people with a rs356219 risk genotype and people with a rs356219 normal genotype, we performed group analyses on the clinical and force measures without covarying for age and sex. Clinical and force data were entered in a multivariate analysis of variance (MANOVA) with genotype (risk vs. normal) as a fixed factor. For the trial by trial analysis of the force data, we used a repeated measures ANOVA with force condition and trial as repeated factors and genotype (risk vs. normal) as between-group factor. All these analyses were considered significant when $p < 0.05$.

For the imaging analyses, the following tests were used: 1) Percent signal change of the task-fMRI signal for the posterior putamen, M1, and angular gyrus was compared between groups using an independent *t*-test with the significance level set at $p < 0.05$. 2) In the functional connectivity analysis, Z-score maps were compared between groups using an independent *t*-test, and because this analysis involved multiple comparisons we corrected the *p* value using AFNI's new ACF approach incorporated in the 3dClustSim function ($p < 0.05$

family-wise error - FWE corrected, minimum cluster size of 12 voxels, voxel size = 3 × 3 × 3 mm). 3) An independent *t*-test was used to compare FW in the posterior substantia nigra between the two groups at $p < 0.05$. 4) The group analysis of GM density was voxel-wise and performed using an independent *t*-test with a multiple comparisons correction at $p < 0.05$ (FWE correction). 5) Similar to the VBM analysis, an independent voxel-wise *t*-test was used to assess group differences in cortical thickness and corrected for multiple comparisons at $p < 0.05$ (FWE correction). For the significant group effects, the effect size was calculated using Hedges' *g*.

3. Results

3.1. Clinical measures

The study sample was in Hardy-Weinberg Equilibrium (HWE) for rs356219 with a X^2 of 0.20. There were no significant differences between individuals with rs356219 risk genotype and individuals with rs356219 normal genotype on any of the clinical, motor and cognitive measures (*p values* > 0.05; Table 1).

3.2. Force measures

Similarly, the force dependent measures (i.e., mean force, rate of force increase, and rate of force decrease) did not differ with genotype (*p values* > 0.05; Table 1). The repeated measures ANOVAs on the trial by trial force data indicated no group differences, condition by group, or trial by group effects for the rs356219 SNP (*p values* > 0.05).

3.3. Imaging measures

3.3.1. Task-based fMRI—Figure 1 shows percent signal change in the two ROIs (posterior putamen, M1) as well as the control ROI (angular gyrus) for the rs356219 genotype groups. The independent *t*-tests revealed significant group differences in the contralateral posterior putamen [$t(29) = 2.596$, $p = 0.015$, Hedges' *g* effect size = 0.943] and contralateral M1 [$t(29) = 2.272$, $p = 0.031$, Hedges' *g* effect size = 0.829], but not in the contralateral angular gyrus ($p = 0.948$). Specifically, the rs356219 risk genotype group had reduced percent signal change in the contralateral posterior putamen and M1 compared to the rs356219 normal genotype group (Table 2).

3.3.2. Task-based functional connectivity—The functional connectivity analyses using the contralateral posterior putamen as a seed showed reduced functional connectivity during grip force between the posterior putamen and cortical motor regions in the rs356219 risk genotype group compared to the rs356219 normal genotype group. The significant cluster is shown in Figure 2 and spanned the contralateral sensorimotor and premotor cortices, with the peak effect in M1 (MNI coordinates: x = -48, y= -18, z = 36; $t = 4.236$; 75 voxels -voxel size = 3 × 3 × 3 mm). No group differences in functional connectivity were found when placing a seed in the contralateral M1.

3.3.3. Free-water diffusion MRI—FW in the posterior substantia nigra did not differ between the rs356219 risk and normal genotype groups ($p = 0.274$) (Table 2).

3.3.4. Voxel-based morphometry—There were no significant differences between the rs356219 risk and normal genotype groups in gray matter density.

3.3.5. Surface-based morphometry—Finally, the two rs356219 genotype groups did not differ in cortical thickness.

4. Discussion

The current study tested the hypothesis that in healthy older adults that carry a PD risk variant for SNCA rs356219, multimodal brain imaging markers of PD differ in comparison to older adults that do not carry a risk variant. There were two key findings. First, we observed reduced fMRI signal during a force control task in the contralateral posterior putamen and contralateral M1 in the group with the risk genotype relative to the group with the normal genotype. Second, when using functional connectivity analysis of the task-based fMRI data, we found that the contralateral posterior putamen had reduced functional connectivity with the contralateral cortical motor areas in carriers of a risk genotype but not in carriers of a normal genotype. These findings were observed in the absence of group differences in clinical measures as well as brain structure as assessed by VBM and SBM, and provide the first evidence that neuroimaging markers from task-fMRI serve as an endophenotype of being a carrier of a PD risk genotype.

SNCA rs356219 has received considerable attention in large-scale genome-wide association studies (Nalls et al., 2014), and its importance for PD risk was also confirmed in various ethnic populations. (Li. et al., 2013; Pan et al., 2012) Alpha-synuclein is a major component of Lewy bodies, which are the pathological hallmark of PD. (Mollenhauer et al., 2011) SNCA rs356219 is a tagging SNP for a disease associated haplotype in the 3′ region of the SNCA gene, and has been shown to influence the level of SNCA mRNA in the substantia nigra and cerebellum. (Fuchs et al., 2008) Importantly, the rs356219 risk allele was also found to be associated with an early onset of PD. (Brockmann et al., 2013) The novelty of this study is that by using a task-fMRI paradigm well-established in PD we were able to study the basal ganglia motor circuit of healthy older adults carrying a PD risk genotype and show that the fMRI signal in the posterior putamen and M1 contralateral to the hand producing force was reduced in people carrying a risk genotype compared to people carrying a low risk genotype. Results are consistent with other task-fMRI studies in the PD literature which demonstrate abnormalities in the putamen and M1 across different stages of PD. (Herz et al., 2013) The fact that force-related activity in the posterior putamen and M1 was reduced in the subjects who carried a risk genotype, without any functional changes in non-PD regions such as the angular gyrus, suggests that functional brain abnormalities across the striato-cortical motor pathway may occur before onset of any motor symptoms. A longitudinal study in PD and parkinsonism found that the fMRI signal during force production in the contralateral putamen and M1 decreased over one year in PD patients but not in the control group, suggesting that these structures become more affected with disease progression. (Burciu, et al., 2016) Interestingly, the task-based functional connectivity analysis using a seed-based approach revealed that the ROI corresponding to the posterior putamen, where the percent signal change effect had been found, had reduced functional connectivity with the cortical motor areas (peak effect in M1). This result suggests that

interactions within the striato-cortical motor network are disrupted in carriers of a rs356219 risk genotype during the performance of a motor task. Of note, fMRI and functional connectivity effects do not appear to be explained by any difficulty in performing the task as both groups showed comparable motor performance inside the scanner. Moreover, we found no differences on other motor tests such as the pegboard and gait tasks, or cognitive status (MOCA score) and BDI depression score. In addition, structural MRI measures derived using VBM, SBM, and FW diffusion MRI did not differ between the two groups. Therefore, structural brain differences are unlikely to have confounded the fMRI results. A recent resting-state fMRI study showed that in asymptomatic LRRK2 G2019S mutation carriers there is a reorganization of cortico-striatal circuits that mirrors changes observed in patients with PD (Helmich et al., 2010). Current findings propose task-based fMRI and task-based functional connectivity as possible endophenotypes for carriers of a PD risk genotype, which could open the door to studying a prodromal cohort in the future. For example, in Alzheimer's disease mild cognitive impairment (MCI) and pre-MCI have become well categorized and are used in clinical research studies to identify prodromal cohorts that may get Alzheimer's disease (Jack et al., 2013). Also, amyloid imaging is being used to assess how novel therapeutics affect amyloid plaques in MCI and pre-MCI cohorts.

In summary, by utilizing neuroimaging to study the genetic variation in the SNP rs356219 of the SNCA gene in older adults, we found an abnormal pattern of functional activity and functional connectivity across the striato-cortical motor pathway in asymptomatic carriers of a PD risk variant. Given that the sample size here is relatively small and can be considered a limitation of the study, future research studies with larger samples are necessary to confirm and extend these findings. Also, future work should include more comprehensive neuropsychological assessments and additional volumetric analyses of the basal ganglia. Studies that incorporate a multimodal approach and follow up a healthy group of people that include carriers and non-carries of PD risk variants longitudinally using imaging and behavioral measurements may provide a cohort of prodromal parkinsonism.

Acknowledgments

The authors would like to thank all participants for their time and commitment to this research, and the National Institutes of Health for funding this study.

Study funding: Supported by the National Institutes of Health (R01NS052318, R01NS075012, T32NS082169), Intramural Research Program of the National Institute on Aging (Z01-AG000949-0).

References

Beck AT, Ward CH, Mendelson M, Mock J, Erbaugh J. An inventory for measuring depression. Archives of general psychiatry. 1961; 4:561–571. [PubMed: 13688369]

Berg D, Postuma RB, Adler CH, Bloem BR, Chan P, Dubois B, Gasser T, Goetz CG, Halliday G, Joseph L, Lang AE, Liepelt-Scarfone I, Litvan I, Marek K, Obeso J, Oertel W, Olanow CW, Poewe W, Stern M, Deuschl G. MDS research criteria for prodromal Parkinson's disease. Mov Disord. 2015; 30(12):1600–1611. [PubMed: 26474317]

Biskup S, Gerlach M, Kupsch A, Reichmann H, Riederer P, Vieregge P, Wullner U, Gasser T. Genes associated with Parkinson syndrome. Journal of neurology. 2008; 255(Suppl 5):8–17. [PubMed: 18787878]

Brockmann K, Schulte C, Hauser AK, Lichtner P, Huber H, Maetzler W, Berg D, Gasser T. SNCA: major genetic modifier of age at onset of Parkinson's disease. Mov Disord. 2013; 28(9):1217–1221. [PubMed: 23674386]

Brooks DJ. Parkinson's disease: diagnosis. Parkinsonism Relat Disord. 2012; 18(Suppl 1):S31–33. [PubMed: 22166447]

Burciu R, Ofori E, Shukla P, Snyder A, Planetta PJ, Hass CJ, Okun MS, McFarland NR, Vaillancourt DE. Distinct patterns of cortical and cerebellar fMRI activity in progressive supranuclear palsy and Parkinson's disease. Movement Disorders. 2015

Burciu RG, Chung JW, Shukla P, Ofori E, Li H, McFarland NR, Okun MS, Vaillancourt DE. Functional MRI of disease progression in Parkinson disease and atypical parkinsonian syndromes. Neurology. 2016; 87(7):709–717. [PubMed: 27421545]

Burciu RG, Ofori E, Archer DB, Wu SS, Pasternak O, McFarland NR, Okun MS, Vaillancourt DE. Progression marker of Parkinson's disease: a 4-year multi-site imaging study. Brain. 2017; 140(8): 2183–2192. [PubMed: 28899020]

Chaudhuri KR, Healy DG, Schapira AH. Non-motor symptoms of Parkinson's disease: diagnosis and management. Lancet neurology. 2006; 5(3):235–245. [PubMed: 16488379]

Chen B, Wang S, Sun W, Shang X, Liu H, Liu G, Gao J, Fan G. Functional and structural changes in gray matter of Parkinson's disease patients with mild cognitive impairment. European journal of radiology. 2017; 93:16–23. [PubMed: 28668411]

Dahnke R, Yotter RA, Gaser C. Cortical thickness and central surface estimation. Neuroimage. 2013; 65:336–348. [PubMed: 23041529]

Desrosiers J, Hebert R, Bravo G, Dutil E. The Purdue Pegboard Test: normative data for people aged 60 and over. Disabil Rehabil. 1995; 17(5):217–224. [PubMed: 7626768]

Fuchs J, Tichopad A, Golub Y, Munz M, Schweitzer KJ, Wolf B, Berg D, Mueller JC, Gasser T. Genetic variability in the SNCA gene influences alpha-synuclein levels in the blood and brain. FASEB journal : official publication of the Federation of American Societies for Experimental Biology. 2008; 22(5):1327–1334. [PubMed: 18162487]

Goetz CG, Tilley BC, Shaftman SR, Stebbins GT, Fahn S, Martinez-Martin P, Poewe W, Sampaio C, Stern MB, Dodel R, Dubois B, Holloway R, Jankovic J, Kulisevsky J, Lang AE, Lees A, Leurgans S, LeWitt PA, Nyenhuis D, Olanow CW, Rascol O, Schrag A, Teresi JA, van Hilten JJ, LaPelle N. Movement Disorder Society-sponsored revision of the Unified Parkinson's Disease Rating Scale (MDS-UPDRS): scale presentation and clinimetric testing results. Mov Disord. 2008; 23(15): 2129–2170. [PubMed: 19025984]

Helmich RC, Derikx LC, Bakker M, Scheeringa R, Bloem BR, Toni I. Spatial remapping of cortico-striatal connectivity in Parkinson's disease. Cereb Cortex. 2010; 20(5):1175–1186. [PubMed: 19710357]

Herz DM, Eickhoff SB, Lokkegaard A, Siebner HR. Functional neuroimaging of motor control in Parkinson's disease: A meta-analysis. Human brain mapping. 2013

Jack CR Jr, Knopman DS, Jagust WJ, Petersen RC, Weiner MW, Aisen PS, Shaw LM, Vemuri P, Wiste HJ, Weigand SD, Lesnick TG, Pankratz VS, Donohue MC, Trojanowski JQ. Tracking pathophysiological processes in Alzheimer's disease: an updated hypothetical model of dynamic biomarkers. Lancet neurology. 2013; 12(2):207–216. [PubMed: 23332364]

Janezic S, Threlfell S, Dodson PD, Dowie MJ, Taylor TN, Potgieter D, Parkkinen L, Senior SL, Anwar S, Ryan B, Deltheil T, Kosillo P, Cioroch M, Wagner K, Ansorge O, Bannerman DM, Bolam JP, Magill PJ, Cragg SJ, Wade-Martins R. Deficits in dopaminergic transmission precede neuron loss and dysfunction in a new Parkinson model. Proc Natl Acad Sci U S A. 2013; 110(42):E4016–4025. [PubMed: 24082145]

Lesage S, Brice A. Role of mendelian genes in “sporadic” Parkinson's disease. Parkinsonism & related disorders. 2012; 18(Suppl 1):S66–70. [PubMed: 22166458]

Li NN, Mao XY, Ghang XL, Zhao DM, Zhang JH, Liao Q, Yu WJ, Tan EK, Peng R. SNCA rs356219 Variant Increases Risk of Sporadic Parkinson's Disease in Ethnic Chinese. Am J Med Genet Part B. 2013; 162B:452–456. [PubMed: 23737253]

Luders E, Thompson PM, Narr KL, Toga AW, Jancke L, Gaser C. A curvature-based approach to estimate local gyrification on the cortical surface. Neuroimage. 2006; 29(4):1224–1230. [PubMed: 16223589]

Mata IF, Shi M, Agarwal P, Chung KA, Edwards KL, Factor SA, Galasko DR, Ginghina C, Griffith A, Higgins DS, Kay DM, Kim H, Leverenz JB, Quinn JF, Roberts JW, Samii A, Snapinn KW, Tsuang DW, Yearout D, Zhang J, Payami H, Zabetian CP. SNCA variant associated with Parkinson disease and plasma alpha-synuclein level. Arch Neurol. 2010a; 67(11):1350–1356. [PubMed: 21060011]

Mata IF, Shi M, Agarwal P, Chung KA, Edwards KL, Factor SA, Galasko DR, Ginghina C, Griffith A, Higgins DS, Kay DM, Kim H, Leverenz JB, Quinn JF, Roberts JW, Samii A, Snapinn KW, Tsuang DW, Yearout D, Zhang J, Payami H, Zabetian CP. SNCA variant associated with Parkinson disease and plasma alpha-synuclein level. Arch Neurol. 2010b; 67(11):1350–1356. [PubMed: 21060011]

Mayka MA, Corcos DM, Leurgans SE, Vaillancourt DE. Three-dimensional locations and boundaries of motor and premotor cortices as defined by functional brain imaging: A meta-analysis. Neuroimage. 2006; 31(4):1453–1474. [PubMed: 16571375]

Mollenhauer B, Locascio JJ, Schulz-Schaeffer W, Sixel-Doring F, Trenkwalder C, Schlossmacher MG. alpha-Synuclein and tau concentrations in cerebrospinal fluid of patients presenting with parkinsonism: a cohort study. Lancet neurology. 2011; 10(3):230–240. [PubMed: 21317042]

Nalls MA, Bras J, Hernandez DG, Keller MF, Majounie E, Renton AE, Saad M, Jansen I, Guerreiro R, Lubbe S, Plagnol V, Gibbs JR, Schulte C, Pankratz N, Sutherland M, Bertram L, Lill CM, DeStefano AL, Faroud T, Eriksson N, Tung JY, Edsall C, Nichols N, Brooks J, Arepalli S, Pliner H, Letson C, Heutink P, Martinez M, Gasser T, Traynor BJ, Wood N, Hardy J, Singleton AB. NeuroX, a fast and efficient genotyping platform for investigation of neurodegenerative diseases. Neurobiology of aging. 2015a; 36(3):1605 e1607–1612.

Nalls MA, McLean CY, Rick J, Eberly S, Hutten SJ, Gwinn K, Sutherland M, Martinez M, Heutink P, Williams NM, Hardy J, Gasser T, Brice A, Price TR, Nicolas A, Keller MF, Molony C, Gibbs JR, Chen-Plotkin A, Suh E, Letson C, Fiandaca MS, Mapstone M, Federoff HJ, Noyce AJ, Morris H, Van Deerlin VM, Weintraub D, Zabetian C, Hernandez DG, Lesage S, Mullins M, Conley ED, Northover CA, Frasier M, Marek K, Day-Williams AG, Stone DJ, Ioannidis JP, Singleton AB. Diagnosis of Parkinson's disease on the basis of clinical and genetic classification: a population-based modelling study. Lancet Neurol. 2015b; 14(10):1002–1009. [PubMed: 26271532]

Nalls MA, Pankratz N, Lill CM, Do CB, Hernandez DG, Saad M, DeStefano AL, Kara E, Bras J, Sharma M, Schulte C, Keller MF, Arepalli S, Letson C, Edsall C, Stefansson H, Liu X, Pliner H, Lee JH, Cheng R, Ikram MA, Ioannidis JP, Hadjigeorgiou GM, Bis JC, Martinez M, Perlmutter JS, Goate A, Marder K, Fiske B, Sutherland M, Xiromerisiou G, Myers RH, Clark LN, Stefansson K, Hardy JA, Heutink P, Chen H, Wood NW, Houlden H, Payami H, Brice A, Scott WK, Gasser T, Bertram L, Eriksson N, Foroud T, Singleton AB. Large-scale meta-analysis of genome-wide association data identifies six new risk loci for Parkinson's disease. Nat Genet. 2014; 46(9):989–993. [PubMed: 25064009]

Nalls MA, Plagnol V, Hernandez DG, Sharma M, Sheerin UM, Saad M, Simon-Sanchez J, Schulte C, Lesage S, Sveinbjornsdottir S, Stefansson K, Martinez M, Hardy J, Heutink P, Brice A, Gasser T, Singleton AB, Wood NW. Imputation of sequence variants for identification of genetic risks for Parkinson's disease: a meta-analysis of genome-wide association studies. Lancet. 2011; 377(9766): 641–649. [PubMed: 21292315]

Nasreddine ZS, Phillips NA, Bedirian V, Charbonneau S, Whitehead V, Collin I, Cummings JL, Chertkow H. The Montreal Cognitive Assessment, MoCA: a brief screening tool for mild cognitive impairment. J Am Geriatr Soc. 2005; 53(4):695–699. [PubMed: 15817019]

Neely KA, Kurani AS, Shukla P, Planetta PJ, Wagle Shukla A, Goldman JG, Corcos DM, Okun MS, Vaillancourt DE. Functional Brain Activity Relates to 0-3 and 3-8 Hz Force Oscillations in Essential Tremor. Cereb Cortex. 2015; 25(11):4191–4202. [PubMed: 24962992]

Neely KA, Planetta PJ, Prodoehl J, Corcos DM, Comella CL, Goetz CG, Shannon KL, Vaillancourt DE. Force control deficits in individuals with Parkinson's disease, multiple systems atrophy, and progressive supranuclear palsy. PLoS One. 2013; 8(3):e58403. [PubMed: 23505500]

Ofori E, Pasternak O, Planetta PJ, Burciu R, Snyder A, Febo M, Golde TE, Okun MS, Vaillancourt DE. Increased free water in the substantia nigra of Parkinson's disease: a single-site and multi-site study. Neurobiol Aging. 2015a; 36(2):1097–1104. [PubMed: 25467638]

Ofori E, Pasternak O, Planetta PJ, Li H, Burciu RG, Snyder AF, Lai S, Okun MS, Vaillancourt DE. Longitudinal changes in free-water within the substantia nigra of Parkinson's disease. Brain. 2015b; 138(Pt 8):2322–2331. [PubMed: 25981960]

Pan F, Dong H, Ding H, Ye M, Liu W, Wu Y, Zhang X, Chen Z, Luo Y, Ding X. SNP rs356219 of the alpha-synuclein (SNCA) gene is associated with Parkinson's disease in a Chinese Han population. Parkinsonism Relat Disord. 2012; 18(5):632–634. [PubMed: 22349157]

Planetta PJ, Kurani AS, Shukla P, Prodoehl J, Corcos DM, Comella CL, McFarland NR, Okun MS, Vaillancourt DE. Distinct functional and macrostructural brain changes in Parkinson's disease and multiple system atrophy. Human brain mapping. 2015; 36(3):1165–1179. [PubMed: 25413603]

Planetta PJ, Ofori E, Pasternak O, Burciu RG, Shukla P, DeSimone JC, Okun MS, McFarland NR, Vaillancourt DE. Free-water imaging in Parkinson's disease and atypical parkinsonism. Brain. 2016; 139(Pt 2):495–508. [PubMed: 26705348]

Prodoehl J, Yu H, Little DM, Abraham I, Vaillancourt DE. Region of Interest Template for the Human Basal Ganglia: Comparing EPI and Standardized Space Approaches. Neuroimage. 2008; 39(3): 956–965. [PubMed: 17988895]

Rektorova I, Biundo R, Marecek R, Weis L, Aarsland D, Antonini A. Grey matter changes in cognitively impaired Parkinson's disease patients. PLoS One. 2014; 9(1):e85595. [PubMed: 24465612]

Rieckmann A, Gomperts SN, Johnson KA, Growdon JH, Van Dijk KR. Putamen-midbrain functional connectivity is related to striatal dopamine transporter availability in patients with Lewy body diseases. Neuroimage Clin. 2015; 8:554–559. [PubMed: 26137443]

Rodriguez S, Gaunt TR, Day IN. Hardy-Weinberg equilibrium testing of biological ascertainment for Mendelian randomization studies. Am J Epidemiol. 2009; 169(4):505–514. [PubMed: 19126586]

Seghier ML. The angular gyrus: multiple functions and multiple subdivisions. Neuroscientist. 2013; 19(1):43–61. [PubMed: 22547530]

Shumway-Cook A, Baldwin M, Polissar NL, Gruber W. Predicting the probability for falls in community-dwelling older adults. Phys Ther. 1997; 77(8):812–819. [PubMed: 9256869]

Spraker MB, Prodoehl J, Corcos DM, Comella CL, Vaillancourt DE. Basal ganglia hypoactivity during grip force in drug naive Parkinson's disease. Human brain mapping. 2010; 31(12):1928–1941. [PubMed: 20225221]

Tessitore A, Giordano A, De Micco R, Russo A, Tedeschi G. Sensorimotor connectivity in Parkinson's disease: the role of functional neuroimaging. Front Neurol. 2014; 5:180. [PubMed: 25309505]

Tzourio-Mazoyer N, Landeau B, Papathanassiou D, Crivello F, Etard O, Delcroix N, Mazoyer B, Joliot M. Automated anatomical labeling of activations in SPM using a macroscopic anatomical parcellation of the MNI MRI single-subject brain. Neuroimage. 2002; 15(1):273–289. [PubMed: 11771995]

- Multimodal non-invasive imaging of healthy individuals with and without the SNCA rs356219 risk genotype
- Reduced functional activity of the putamen and primary motor cortex in carriers of a risk genotype
- The putamen presents abnormal functional connectivity with cortical motor brain regions in carriers of a risk genotype

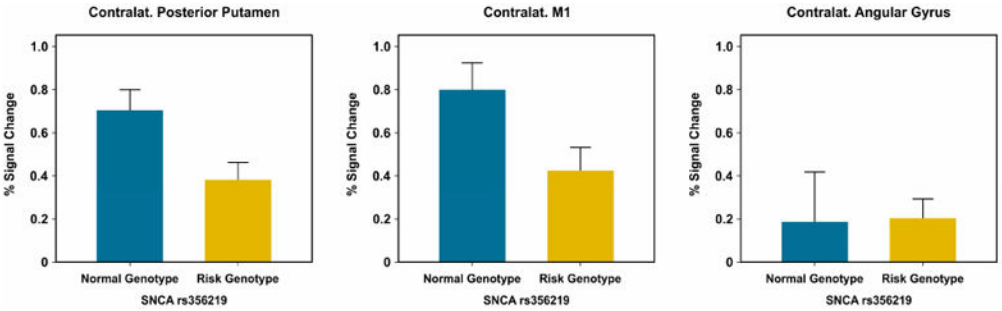

Figure 1.

Percent signal change for the contralateral posterior putamen, M1, and angular gyrus, plotted for the risk genotype and normal genotype groups. Data are mean +1 standard error.

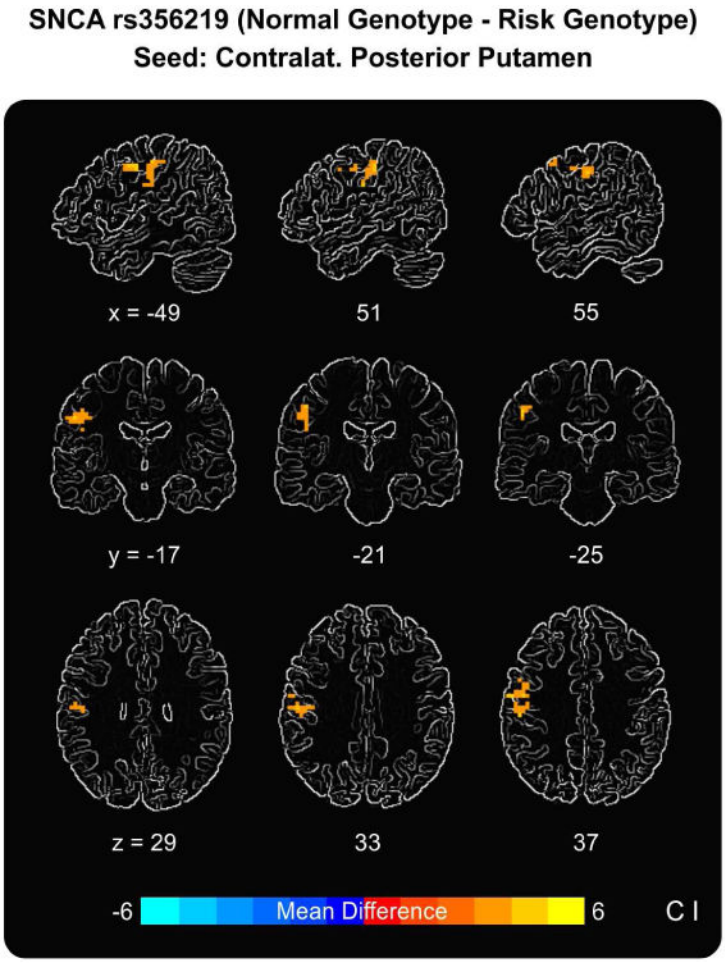

Figure 2.

Task-based functional connectivity results using the contralateral posterior putamen as a seed. Results show reduced functional connectivity during grip force between the contralateral posterior putamen and a cluster in the contralateral cortical motor areas (peak in M1) in the risk genotype group compared to the normal genotype group.

Table 1

Demographics & Behavior	SNCA rs356219		P-Value
	Normal Genotype	Risk Genotype	
Sample, N	13	18	N/A
Age, Yrs	64.08 (9.66); Range: 47-81	60.83 (9.05); Range: 48-76	0.347
Gender, M|F	6|7	8|10	0.925
Hand tested, L|R	7|6	8|10	0.605
MDS-UPDRS-III	3.69 (3.72)	2.61 (2.57)	0.579
Purdue Pegboard Test	20.00 (3.21)	20.83 (3.80)	0.537
Dynamic Gait Index	23.62 (0.65)	23.11 (1.23)	0.291
MoCA	26.54 (1.89)	27.06 (2.41)	0.318
Beck Depression Inventory	3.77 (4.58)	2.83 (3.14)	0.598
Mean force, % MVC	14.92 (4.04)	14.88 (6.11)	0.983
Rate-up, N/s	25.79 (10.64)	23.68 (11.57)	0.610
Rate-down, N/s	-39.65 (17.90)	-46.37 (21.75)	0.369

Data are count, or mean ± SD. Abbreviations: F = female, L = left, M = male, MDS-UPDRS-III = Movement Disorder Society Unified Parkinson's Disease Rating Scale, MoCA = Montreal Cognitive Assessment, MVC = maximum voluntary contraction, N/s = Newton per second, R = right, Yrs = years.

Neurobiol Aging. Author manuscript; available in PMC 2019 June 01.

Table 2

Imaging	SNCA rs356219	
	Normal Genotype	Risk Genotype
% Signal Change: Posterior Putamen	0.70 (0.34)	0.38 (0.34)
% Signal Change: M1	0.80 (0.44)	0.42 (0.45)
% Signal Change: Angular Gyrus	0.18 (0.83)	0.20 (0.38)
FW: Posterior Substantia Nigra	0.18 (0.04)	0.20 (0.05)

Abbreviations: FW = free-water, M1 = primary motor cortex.